ISSN 1063-7842, Technical Physics, 2016, Vol. 61, No. 9, pp. 1346–1351. © Pleiades Publishing, Ltd., 2016.
Original Russian Text © B.V. Petukhov, 2016, published in Zhurnal Tekhnicheskoi Fiziki, 2016, Vol. 86, No. 9, pp. 65–70.

SOLID STATE

Dynamic Strain Aging of the Materials Characterized by the Peierls Plasticity Mechanism

B. V. Petukhov

Institute of Crystallography, Russian Academy of Sciences, Leninskii pr. 59, Moscow, 119333 Russia

e-mail: petukhov@ns.crys.ras.ru

Received November 3, 2015

Abstract—A synergetic model is proposed to describe the influence of dynamic strain aging on the plasticity of materials that is controlled by the Peierls barriers overcome by dislocations. The immobilization of dislocations by the impurities concentrated in the dislocation cores is taken into account. The behavior of calculated deformation curves is studied as a function of the material parameters and the mechanical test conditions.

DOI: 10.1134/S1063784216090188

INTRODUCTION

A widely used method of studying the mechanical properties of materials is to measure their deformation curves at a given constant strain rate $\dot{\varepsilon}$, i.e., the change required to maintain stress with time t (or, what is equivalent, with strain $\varepsilon = \dot{\varepsilon} t$). The deformation curves are then processed using basic models to extract the quantitative characteristics of deformation mechanisms, such as the dynamics of dislocations. The influence of uncontrollable impurities often distorts experimental results. Therefore, it is useful to determine the involvement of impurity effects from the qualitative shape of the deformation curves. This brings up the problem of describing the qualitative changes in the deformation curves that are caused by the impurity subsystem in a crystal.

The tendency of dislocation cores to be covered with impurities leads to the modification of the dynamic behavior of dislocations, i.e., so-called "aging." On a macroscopic level, dislocation aging manifests itself in material hardening, a change in the strain-rate sensitivity of deforming stress, anomalies in the temperature dependence of the yield point, and serrated plastic flow [1, 2]. In general, these phenomena are called dynamic strain aging (DSA) of a material.

The plasticity of materials is often described in terms of a mechanical approach using phenomenological equations, which are derived to reproduce certain experimental results [3]. However, in essence, DSA is a memory process; therefore, it is difficult to find a correct set of equations using a purely phenomenological approach. In this case, it is helpful to apply the physical concepts of plastic flow as dislocation motion through the potential barriers induced by the microstructure of the material. The advantage of such an approach is the possibility of taking into account the specific features of materials with various dislocation mobility mechanisms. The theories of diffusion impurity motion to cores when a thermal fluctuation, which throws a dislocation segment over an obstacle, is waited for are widely applied to the materials where dislocation motion is controlled by local obstacles [4, 5]. In these time intervals, static aging of dislocation segments actually takes place. Dislocation segments jump over a significant distance, which is larger than the interatomic distance; therefore, the trapping of detachable impurities and the history of impurity accumulation in dislocation cores may be neglected. A detailed description of the physical foundations of such theories and numerous references are given in review [6]. Models are developed to describe the specific features of plastic flow that are related to the N-shaped strain-rate sensitivity of the dislocation drag that appears under certain conditions (see, e.g., [7]). DSA models for the materials where the dislocation mobility is controlled by the potential relief of the crystal lattice, so-called Peierls barriers, with the period that is equal to the lattice parameter are less developed. These materials include covalent crystals, bcc metals, and intermetallics [1, 2]. The purpose of this work is to develop a DSA theory for such materials, where jumplike dislocation motion manifests itself on a microscopic scale and is considered to be continuous on a larger scale. Strictly speaking, dislocation aging has a dynamic nature only in this case.

SYNERGETIC MODEL FOR THE PLASTICITY OF AN IDEAL CRYSTAL DUE TO DISLOCATION MOTION AND MULTIPLICATION IN AN ENSEMBLE

As a starting base, we consider a deformation model for a perfect crystal with a negligibly low impurity content [8, 9]. Total strain rate $\dot{\varepsilon}$ is the sum of elastic $(1/S)d\sigma/dt$ and plastic $NbV(\sigma_{ef})$ components,

$$(1/S)d\sigma/dt = \dot{\varepsilon} - NbV(\sigma_{ef}). \quad (1)$$

Here, σ is the applied stress, S is the elastic modulus, t is the time, N is the dislocation density, b is the Burgers vector, V is the dislocation velocity, and σ_{ef} is the effective stress (i.e., external stress σ modified by internal stresses of various natures). The stress dependence of the velocity is described as $V(\sigma_{ef}) = B\sigma_{ef}^m$, where B is the dislocation mobility and m is the experimental strain-rate sensitivity.

Following [8, 9], we describe the dislocation self-multiplication ability by the empirical law

$$dN/dt = w\sigma_{ef}^n V(\sigma_{ef})N, \quad (2)$$

where parameters w and n are varied from material to material. Equation (2) is often supplemented with the terms that describe dislocation annihilation [1, 6, 10]. In this work, however, we do not use these terms because of the assumption that the density of mobile dislocations is relatively low in the vicinity of the yield strength under study.

Equations (1) and (2) were successfully applied to describe the deformation of alkali-halide and semiconductor crystals [8–14]. The models applied to various materials are classified in terms of exponents m and n in the stress dependences in Eqs. (1) and (2). To describe the phenomenon of dynamic strain aging, we have to generalize a theory by taking into account the interaction of a dislocation ensemble with the impurity subsystem of a crystal.

DYNAMIC STRAIN AGING

Dislocation cores have energetically predominant sites for impurities. As a result, dislocations attract impurities, and they either diffuse into the dislocation cores or are trapped by them during contact in the course of dislocation motion in a crystal. The impurities located in a dislocation core adhere to the crystal lattice, which decreases the force moving the dislocation. The amount of impurities accumulated in a dislocation core depends on the nucleation time of the dislocation and its lifetime (age) under variable external conditions, which assigns a literal meaning to the concept of aging. Thus, the dynamics of a dislocation ensemble in an impurity-containing material has specific memory of individual history of dislocation motion [14, 15]. This fact means that, strictly speaking, deformation should be described by time-nonlocal relations, which is not taken into account in most phenomenological approaches. Below, we develop a model to take into account different dislocation ages in an ensemble, which is a necessary ingredient for an adequate description of deformation.

For this purpose, we will use a differential dislocation density, namely, dislocation generation rate $\rho(t)$ in a time interval from t to $t + dt$, rather than a total dislocation density. The increment of the total dislocation density ΔN in time dt is $\Delta N = \rho(t)dt$. The total density by time t is the sum of contributions generated at various previous times. As a result, we have modified Eq. (2),

$$\rho(t) = wN_0\sigma_{ef}^n(t)V[\sigma_{ef}(t)] + w\int_0^t dt_1\rho(t_1)\sigma_{ef}^n(t,t_1)V[\sigma_{ef}(t,t_1)] = wBN_0\sigma_{ef}^{n+m} + wB\int_0^t dt_1\rho(t_1)\sigma_{ef}^{n+m}(t,t_1), \quad (3)$$

where N_0 is the initial dislocation density and t_1 is the time of nucleation of new dislocations. Similarly, Eq. (1) for the deforming stress changes,

$$(1/S)d\sigma/dt = \dot{\varepsilon} - bN_0V[\sigma_{ef}(t)] - b\int_0^t dt_1\rho(t_1)V[\sigma_{ef}(t,t_1)] = \dot{\varepsilon} - bBN_0\sigma_{ef}^m - bB\int_0^t dt_1\rho(t_1)\sigma_{ef}^m(t,t_1). \quad (4)$$

Equations (3) and (4) illustrate the memory of dislocations about evolution in the previous times of their "biographies."

The motion of a dislocation in an impurity-containing crystal is damped in time due to an increase in the impurity content in its core, and deformation is maintained owing to the nucleation of "fresh" dislocations. For example, the Ananthakrishna theory [6] takes into account the influence of impurity atoms on a decrease in the density of mobile dislocations by setting the rate of this process in the entire ensemble. The model proposed in this work takes into account the individual impurity accumulation kinetics in a dislocation core to a certain extent, which is achieved by taking into account the external stress operating during dislocation nucleation. The subsequent aging of a dislocation is simulated a gradual decrease in the effective stress moving the dislocation from its nucleation.

We consider the situation when dislocation kinetics occurs at the times that are short as compared to the kinetics of the entire dislocation ensemble. The immobilization of an individual dislocation is simulated using a decreasing effective stress on it,

$$\sigma_{ef}(t,t_1) = \sigma(t)\exp[-(t-t_1)/\tau_{im}], \quad (5)$$

where t is the current time, t_1 is the dislocation nucleation time, and τ_{im} is the average immobilization time determined by the rate of impurity accumulation in a dislocation core. When a dislocation nucleates ($t = t_1$), it has no excess impurities and the effective stress on it is equal to external stress $\sigma_{ef}(t, t_1) = \sigma(t)$. When the dislocation age $t - t_1$ increases, the effective stress decays because of an increasing impurity content in the dislocation core and the related drag force. Time τ_{im} is considered to be short as compared to the time of changing stress $\sigma(t)$. The immobilization kinetics is determined by the following factors: impurity concentration c_0 in a crystal, the force of impurity–dislocation interaction, and so on. For example, when impurities are completely trapped in a layer of thickness r, τ_{im} was estimated to be $\tau_{im} \sim a^2/(rB\beta c_0)$ [14, 15]. Here, β is the coefficient of proportionality between the impurity content at a dislocation and the generating retarding stress. Thus, using parameter τ_{im}, we describe the combined influence of these factors on deformation.

Leaving aside some secondary side phenomena, such as strain hardening, we study the possible types of manifestation of dynamic dislocation aging in the plastic flow kinetics in various (m, n) models. Strain hardening can be approximately taken into account as an additional additive contribution to the internal stresses, which does not change qualitative conclusions.

Deformation curves can have the so-called yield drop, where the deforming stress changes abruptly and then behaves evenly. The calculation by Eqs. (3)–(5) shows that the yield drop height, which is called the upper yield stress, and the yield drop width are substantially modified in impurity-containing crystals as compared to the corresponding pure crystals. The figures presented below illustrate these changes. However, the most pronounced changes in the deformation curves are caused by dynamic dislocation aging at the stage following the yield point.

STATIONARY STATE

A stationary state can be reached during deformation, and the conditions of this state will analyzed below. In the stationary state, the stress and the rate of dislocation generation become constant, $\sigma = \sigma_s$ and $\rho = \rho_s$, respectively. Substituting these constants into Eqs. (3)–(5) and taking the time integral, we obtain their values

$$\sigma_s = \left(\frac{n+m}{wB\tau_{im}}\right)^{1/(n+m)}, \qquad \rho_s = \frac{\dot{\varepsilon}m}{bB\tau_{im}}\left(\frac{wB\tau_{im}}{n+m}\right)^{m/(n+m)} \quad (6)$$

in the limit $t \to \infty$.

The obtained stationary stress can be compared to the analogous value calculated by the full impurity trapping model [14, 15] for the case $m = 1$, $\sigma = [(n + 1)\beta c_0 r/(wa^2)]^{1/(n+1)}$, and find that they agree with each other at the value of immobilization time τ_{im} given above. It is interesting that the impurity contribution to deforming stress (6) is independent of strain rate ε.

Below, we will present slightly different equations of the model, which are more convenient for calculations and studying the stability of the stationary state. We substitute the explicit time dependence of the effective stress (Eq. (5)) into Eq. (3), divide both parts of the equation by $\sigma^{n+m}\exp[-(n+m)t/\tau_{im}]$, differentiate it with respect to time, and obtain

$$\sigma\dot{\rho} - (n+m)\rho\sigma + (n+m)\rho\sigma/\tau_{im} - wB\rho\sigma^{n+m+1} = 0. \quad (7)$$

Applying a similar procedure to Eq. (4), we reduce it to the form

$$\sigma\ddot{\sigma} - m\dot{\sigma}(\dot{\sigma} - S\dot{\varepsilon}) + m\sigma(\dot{\sigma} - S\dot{\varepsilon})/\tau_{im} + bBS\rho\sigma^{m+1} = 0. \quad (8)$$

It is seen that Eqs. (7) and (8) have the same stationary solution (Eq. (6)), as would be expected.

MODES OF REACHING THE STATIONARY STATE AND THE CRITERION OF ITS STABILITY

The aim of this section is to study the shape of deformation curves outside the yield strength as a function of the problem parameters, first of all, exponents m and n. Using the set of differential equations (7) and (8), we analyze the behavior of the curves near stationary solution (6) in the approximation that is linear in deviation on the assumption that $\rho = \rho_s + \delta\rho$ and $\sigma = \sigma_s + \delta\sigma$. To this end, we use the following scale factors: S for stress, $t_0 = 1/(wBS^{m+n})$ for time, $\rho_0 = (1/b)w^2BS^{m+2n}$ for the dislocation generation rate, $\rho_0 t_0$ for the dislocation density, and dimensionless parameters $\varepsilon = \dot{\varepsilon}t_0$ and $\tau = \tau_{im}/t_0$.

To study the stability of the stationary solution, the time dependence of the deviation is sought for in the form $\delta\rho$ and $\delta\sigma \sim \exp(\lambda t/\tau)$. The following characteristic equation is derived in a standard manner:

$$\lambda^3 + a_1\lambda^2 + a_2\lambda + a_3 = 0, \quad (9)$$

where $a_1 = (m + u)$, $a_2 = (n + 2m)u$, $a_3 = (n + m)^2u$, and $u = m\varepsilon\tau/\sigma_s$.

The stationary state is stable if the deviations $\delta\rho$ and $\delta\sigma \sim \exp(\lambda t/\tau)$ from it decrease in time, which takes place when the real parts of all solutions to the characteristic equation are negative. According to the well-known criterion for a cubic equation (see, e.g., [17]), this situation occurs at $a_1a_2 > a_3$, i.e., at $u > \frac{n^2 + nm - m^2}{n + 2m}$ in our case. If $n \le \frac{\sqrt{5}-1}{2}m$, the right-hand side is negative or zero and the stationary state is

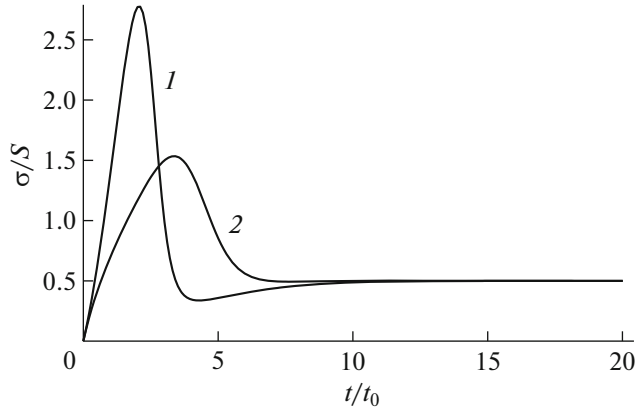

Fig. 1. Deformation curves for parameters $n = 0$, $m = 1$, $\tau = 2$, and $\varepsilon = (1)$ 0.99 and (2) 1.01.

stable at any other parameters. For example, at $n = 0$, the stationary state is stable at any nonnegative m. This conclusion agrees with the shape of the deformation curves calculated by Eqs. (7) and (8) and illustrated in Fig. 1. The limitation imposed on u to achieve stability takes place at $n > \frac{\sqrt{5}-1}{2}m$. For example, at $n = 1$ and $m = 1$, we have $u = \varepsilon\tau^{3/2}/\sqrt{2} > 1/3$ for stability. In this case, the deformation curve has the shape shown in Fig. 2a and the stationary state is reached via damped oscillations. At $\varepsilon\tau^{3/2}/\sqrt{2} \le 1/3$, the stationary state is unstable and continuous oscillations take place instead of it (see Fig. 2b).

We now find the condition of oscillations in the deformation curves during uniform deformation. Oscillations are absent when all three roots of the characteristic equation are real. In the trivial case at $n = 0$, the characteristic equation can easily be solved and have the roots $\lambda_3 = -m$ and $\lambda_{1,2} = \frac{1}{2}\{-u \pm (u^2 - 4mu)^{1/2}\}$. The roots are real at $u(= m^{1-1/m}\varepsilon t^{1+1/m}) \ge 4m$. At $u < 4m$, oscillations can occur in the deformation curves. The calculation demonstrates that oscillations are present in this case; however, their amplitude is low and they manifest themselves in the minimum behind the yield drop in Fig. 1.

Let us consider the general case at $n > 0$. At low u, one real negative root ($\lambda_3 \approx -m$) takes place and two other roots have imaginary parts, $\lambda_{1,2} \approx -u/2 \pm i(mu)^{1/2}$. At high u, one root is high and negative ($\lambda_3 \approx -u$) and two other roots are

$$\lambda_{1,2} \approx \frac{1}{2}\{-(n+2m)\} \pm i[3n^2 + 4nm]^{1/2}\}. \qquad (10)$$

Thus, at n, $m > 0$, the roots can be real only in a limited intermediate u range. The theory of cubic equations asserts that the types of solution are classified with the discriminant [17]

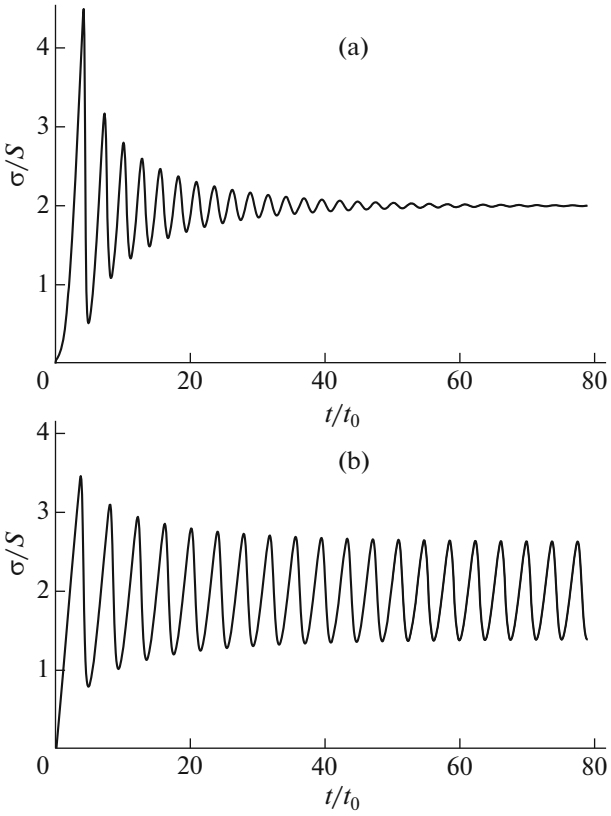

Fig. 2. Deformation curves for parameters $n = 1$, $m = 1$, $\tau = 0.5$, and $\varepsilon =$ (a) 2 and (b) 0.5.

$$\begin{aligned} D = a_1^2a_2^2 - 4a_2^3 - 4a_1^3a_3 - 27a_3^2 + 18a_1a_2a_3 \\ = -n(3n+4m)u^3 + (14n^2 + 38nm + 26m^2)nu^2 \\ + (-27n^4 - 90n^3m - 101n^2m^2 \\ - 38nm^3 + m^4)u - 4(n+m)^2m^3 \end{aligned} \qquad (11)$$

and are represented by the following three types:

$D > 0$, the equation has three different real roots;

$D < 0$, the equation has one real and two complex-conjugate roots;

$D = 0$, the equation has three real roots, at least two of them being coincident.

Thus, the boundary between the oscillating and the monotonic behavior of the deformation curves beyond the yield point is determined by the condition $D = 0$. If this boundary exists, it can be calculated by Eq. (11). For illustration, the result of this calculation for $n = 1$ and arbitrary m is shown in Fig. 3. At the parameters corresponding to region *1* between boundaries u_1 and u_2, monotonic behavior of the deformation curves is expected, and oscillating behavior should occur in other cases.

Figure 4 depicts phase diagrams for the types of solution for the model at $m = n = 1$ that exist at the values of control parameter u on either side of the critical

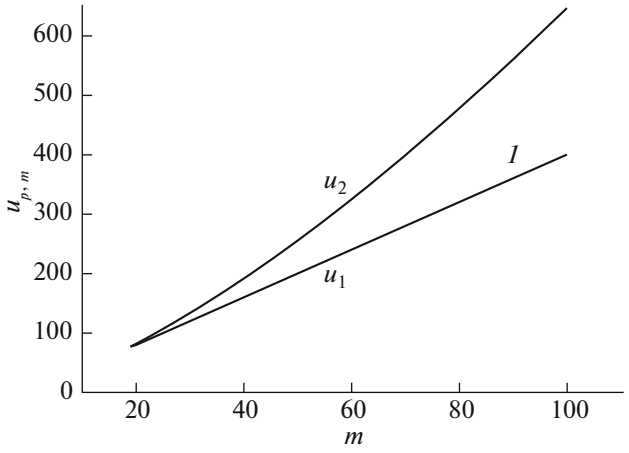

Fig. 3. Parameter regions where (*1*) monotonic and outside of which oscillating behavior of deformation curves beyond the yield point takes place.

value (1/3): a stable focus is seen at $D > 0$ (Fig. 4a, $u = 1$) and a limiting cycle, at $D < 0$ (Fig. 4b, $u = 0.2$).

DISCUSSION OF RESULTS

The interaction of dislocations with the impurity subsystem of a material substantially affects its mechanical properties, in particular, plasticity. Leaving aside strain hardening, the model of the deformation of a pure material that is represented by Eqs. (1) and (2) results in monotonic stable behavior of deformation curves outside the yield point. The generalized model developed for alloyed materials and alloys takes into account the effect of the impurity subsystem and leads to a larger variety of the types of deformation curves. The stationary state outside the yield point can be reached monotonically and after a series of damped oscillations. Moreover, the stationary state cannot be reached at certain parameters, and continuous stress oscillations occur instead of it. These oscillations can be considered as the precursor of the appearance of nonuniform plastic-flow instabilities, such as the Portevin–Le Chatelier effect [6], and correspond to the experimentally detected types of behavior of doped silicon crystals [18].

The specific features in the temperature and strain-rate dependences of the deforming stress are considered as characteristic signs of DSA in the works dealing with mechanical tests [19]. The weakening of the strain-rate sensitivity that was experimentally detected in alloyed crystals can be explained in terms of the substantial impurity contribution described by Eq. (6) and independent of the strain rate. The presence of oscillations in stress–strain curves can be a direct indication of dynamic strain aging. For convenience of extraction of the temperature and strain-rate dependences of the deforming stress, the oscillations in deformation curves are often smoothed for the models

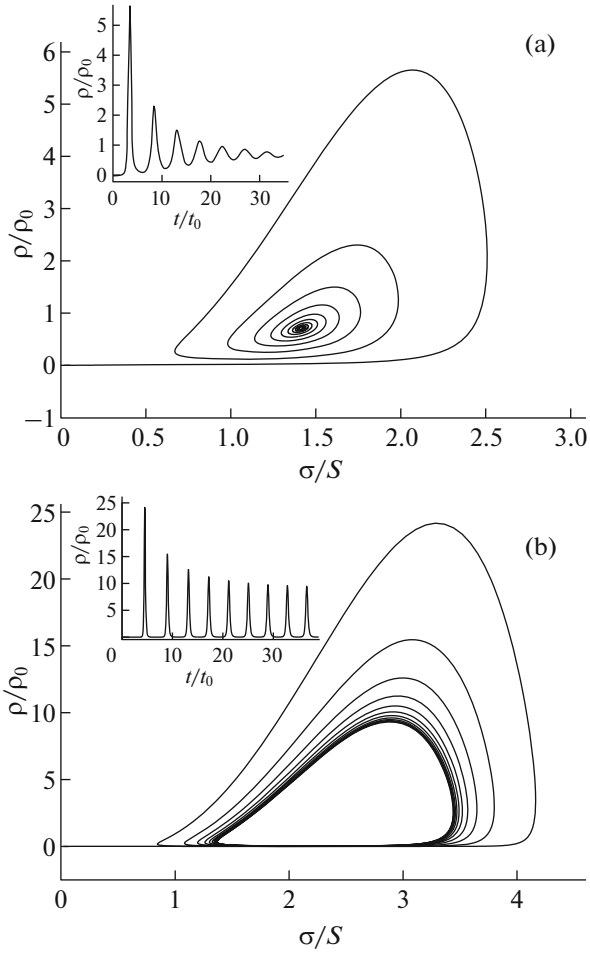

Fig. 4. Phase portrait of the solutions to the model equations at $m = n = 1$, which demonstrates the behavior of dislocation generation rate ρ at a control parameter $u =$ (a) 1 and (b) 0.2. (insets) Time evolution of ρ.

related to impurity-free materials to be applied [20]. This approach is valid and attractive due to the simplicity of application. However, the theory developed in this work can serve as the basis for a more adequate analysis of experimental data.

REFERENCES

1. U. Messerschmidt, *Dislocation Dynamics during Plastic Deformation,* Springer Series in Material Science, Ed. by R. Hull, C. Jagadish, R. M. Osgood, J. Parisi, Jr., Z. Wang, and H. Warlimont (Heidelberg, New York, 2010).
2. E. Nadgorny, Progr. Mater. Sci. **31**, 1 (1988).
3. R. Akhtar and S. Khan, Int. J. Plasticity **15**, 963 (1999).
4. M. A. Lebedkin and L. R. Dunin-Barkovskii, JETP **86**, 993 (1998).
5. M. A. Lebyodkin, T. A. Lebedkina, F. Chmelk, T. T. Lamark, Y. Estrin, C. Fressengeas, and J. Weiss, Phys. Rev. B **79**, 174114 (2009).
6. G. Ananthakrishna, Phys. Rep. **440** (4–6), 113 (2007).

7. V. V. Malashenko, Phys. Solid State **57**, 2461 (2015).
8. W. G. Johnston and J. J. Gilman, J. Appl. Phys. **30** (2), 129 (1959).
9. H. Alexander, *Dislocations in Solids,* Ed. by F. R. N. Nabarro (North-Holland, Amsterdam, 1986), Vol. **7**, Chap. 35, pp. 113–235.
10. G. A. Malygin, Phys. Usp. **42**, 887 (1999).
11. J. Cochard, I. Yonenaga, S. Gouttebroze, M. M'Hamdi, and Z. L. Zhang, J. Appl. Phys. **108**, 103524 (2010).
12. M. Suezawa, K. Sumino, and I. Yonenaga, Phys. Status Solidi A **51** (1), 217 (1979).
13. J. Rabier and A. George, Rev. Phys. Appl. **22**, 1327 (1987).
14. B. V. Petukhov, Tech. Phys. **46**, 1389 (2001).
15. B. V. Petukhov, Tech. Phys. **48**, 880 (2003).
16. B. V. Petukhov, Phys. Status Solidi C **2**, 1864 (2005).
17. I. N. Bronshtein and K. A. Semendyaev, *A Handbook of Mathematics* (Nauka, Moscow, 1986).
18. H. Siethoff, Acta Metall. **21**, 1523 (1973).
19. T. S. Gross, V. K. Mathews, R. J. De Angelis, and K. Okazaki, Mater. Sci. Eng. A **117** (9), 75 (1989).
20. R. Kapoor and S. Nemat-Nasser, Metall. Mater. Trans. A **31**, 815 (2000).

Translated by K. Shakhlevich